

Nonlinear Evolution of Very Small Scale Cosmological Baryon Perturbations at Recombination

Guo-Chin Liu^{1,2)}, Kazuhiro Yamamoto³⁾, Naoshi Sugiyama¹⁾, and Hiroaki Nishioka³⁾

¹⁾Division of Theoretical Astrophysics, National Astronomical Observatory Japan, Mitaka, 181-8588, Japan

²⁾Department of Physics, Kyoto University, Kyoto 606-8502, Japan

³⁾Department of Physics, Hiroshima University, Higashi-Hiroshima 739-8526, Japan

ABSTRACT

The evolution of baryon density perturbations on very small scales is investigated. In particular, the nonlinear growth induced by the radiation drag force from the shear velocity field on larger scales during the recombination epoch, which is originally proposed by Shaviv in 1998, is studied in detail. It is found that inclusion of the diffusion term which Shaviv neglected in his analysis results in rather mild growth whose growth rate is $\ll 100$ instead of enormous amplification $\sim 10^4$ of Shaviv's original claim since the diffusion suppresses the growth. The growth factor strongly depends on the amplitude of the large scale velocity field.

The nonlinear growth mechanism is applied to density perturbations of general adiabatic cold dark matter (CDM) models. In these models, it has been found in the previous works that the baryon density perturbations are not completely erased by diffusion damping if there exists gravitational potential of CDM. With employing the perturbed rate equation which is derived in this paper, the nonlinear evolution of baryon density perturbations is investigated. It is found that: (1) The nonlinear growth is larger for smaller scales. This mechanism only affects the perturbations whose scales are smaller than $\sim 10^2 M_\odot$, which are coincident with the stellar scales. (2) The maximum growth factors of baryon density fluctuations for various COBE normalized CDM models are typically less than factor 10 for $3 - \sigma$ large scale velocity peaks. (3) The growth factor depends on Ω_b .

Subject headings: cosmology: theory

1. INTRODUCTION

Structure formation of the universe from the large scale structure to the stellar objects is one of the most important issues of modern cosmology and astrophysics. Within a framework of

the hierarchical clustering scenario which is suggested by the adiabatic cold dark matter (CDM) models, formation of first luminous objects in the universe has been discussed by many authors (e.g., Fukugita & Kawasaki 1994; Gnedin & Ostriker 1997; Ostriker & Gnedin 1996; Haiman & Loeb 1997; Nishi, et al 1998). According to those theoretical investigations, in which the initial dark matter and baryon density fluctuations have been solved linearly, the first luminous objects are thought to appear in the gas clouds in the dark halo at $z \sim a \text{ few} \times 10$, depending on the cosmological models.

On the other hand a new mechanism which causes rapid growth of the baryon density fluctuations on very small scales during a short period of the recombination epoch has been proposed by Shaviv (1998). This growth of the baryon density perturbations is caused by the radiation drag force from the large scale velocity field which is coupled to the small scale baryon perturbations in a nonlinear manner. He has pointed out enormous growth ($\sim 10^4$) of baryon fluctuations if the wavelength of the perturbations is shorter than a critical value. Such enormous amplification of baryon density fluctuations must lead to early formation of stellar objects. If the amplification is as large as Shaviv's prediction, therefore, it might be a quite interesting antithesis for the standard scenario of the cosmic structure formation in the CDM cosmological models, though we will show that this nonlinear growth mechanism would not be so drastic.

In this paper, we first carefully re-examine Shaviv's treatment of density perturbations. We find the diffusion term which Shaviv has neglected in his analysis plays a crucial role for suppression of the nonlinear growth.

There are also some artificial assumptions in Shaviv's investigation. First one is in use of the thermal equilibrium for the recombination process. This nonlinear growth is induced by the shear velocity field on larger scales through the radiation drag force against density fluctuations of ionized hydrogens. Therefore we need to calculate fluctuations of the ionization fraction. Shaviv has obtained these fluctuations by employing the perturbed Saha equation which should not be applied during the recombination epoch. Here we develop a new method to treat these fluctuations by the perturbed treatment of the rate equation which is an extension of the previous work by Yamamoto, Sugiyama, and Sato (1997, Paper I).

The next assumption Shaviv has made in his investigation is the existence of isothermal baryon density fluctuations. It is well known that the adiabatic baryon and photon density perturbations are erased away due to the photon diffusion before and during the recombination epoch (Silk 1968; Sato 1971; Weinberg 1971). The diffusion (Silk) damping scale goes over the galaxy scale. Therefore it seems to be unavoidable for the nonlinear growth mechanism to assume small scale isothermal baryon perturbations during the recombination epoch as the seeds of baryon perturbations in an artificial manner. The origin of the small scale isothermal baryon perturbations has not been considered.

However we would like to stress that the small scale isothermal baryon density fluctuations are produced after the Silk damping in general CDM cosmological models without any ad hoc

assumptions. Such isothermal baryon density fluctuations on small scales have been found by Yamamoto, Sugiyama & Sato (1998, Paper II). Once baryon fluctuations are damped by diffusion. However they grow again owing to the gravitational potential of CDM before the recombination epoch due to the breakdown of the tight-coupling between baryons and background photons. Since the Compton drag from background photons is still effective at that epoch and works as friction, this growth of baryon density fluctuations is characterized by the terminal velocity. Such natural existence of the small scale isothermal baryon density fluctuations motivates us to revisit Shaviv’s investigation in the context of the conventional adiabatic CDM models.

The paper is organized as follows: In §2, we review the nonlinear growth mechanism which Shaviv has proposed. Some numerical tests for a toy model with simple assumptions are presented in §3. It is shown that the diffusion term plays a crucial role for the estimate of the growth factor. In §4, we examine whether the nonlinear growth mechanism is effective on the adiabatic CDM models or not. §5 is devoted to summary. Throughout this paper we work in units where $c = \hbar = k_B = 1$, and assume $T_0 = 2.726$ K as the cosmic microwave radiation temperature at present.

2. Basic Equations for the Nonlinear Effect

Before describing the nonlinear growth mechanism of small scale baryon density fluctuations proposed by Shaviv (1998), let us first summarize basic equations (see also Paper I; II). We work in the Newtonian perturbed metric,

$$ds^2 = \left(\frac{a}{a_0}\right)^2 \left(- (1 + 2\Psi)d\eta^2 + (1 - 2\Psi)d\mathbf{x}^2\right), \quad (1)$$

where Ψ is the perturbed gravitational potential, a is the scale factor whose suffix 0 indicates the present value, and $\eta \equiv \int dt(a_0/a)$. As we are interested in the small scale cosmological perturbations, we can assume the geometry of the universe to be flat. Then, in the high redshift universe, the Friedmann equation leads to

$$H^2 = \left(\frac{\dot{a} a_0}{a}\right)^2 = \left(\frac{a_0}{a}\right)^4 \frac{a_{\text{eq}} + a}{a_{\text{eq}} + a_0} \Omega_0 H_0^2, \quad (2)$$

where the dot denotes η -differentiation, H_0 is the Hubble constant, and a_{eq} is the scale factor at the matter-radiation equality epoch which can be written as

$$\frac{a_0}{a_{\text{eq}}} = 4.04 \times 10^4 (1 - f_\nu) \Omega_0 h^2, \quad (3)$$

with f_ν being the neutrino fraction in the energy density of radiation components. For the massless standard neutrino model with three species, $f_\nu \simeq 0.405$, which we adopt throughout the present paper. Here, we take into account the fraction of helium abundance. Hence we define the fractional ionization x_e as

$$x_e \equiv \frac{n_e}{2n_{\text{He}} + n_{\text{H}}}, \quad (4)$$

where n_e , n_{He} , and n_{H} are the number densities of free electron, helium, and hydrogen, respectively. The primordial helium mass fraction is defined as

$$y_p \equiv \frac{4n_{\text{He}}}{n_{\text{b}}}, \quad (5)$$

where $n_{\text{b}} \equiv 4n_{\text{He}} + n_{\text{H}}$ is the net baryon number density. We set $y_p = 0.24$ throughout the present paper. The fractional ionization x_e is 1 in the very early universe and becomes $(1 - y_p)/(1 - y_p/2) \simeq 0.86$ just before the recombination epoch due to the early recombination of helium atoms.

Let us now describe the nonlinear growth mechanism. We proceed with reviewing equations of the small perturbations for the baryon-electron fluid. Since we are interested in the evolution of density perturbations on very small scales, we adopt the Newtonian approximation. The evolution equations for the baryon-electron fluid coupled with the primeval radiation through Compton scattering are written as

$$\dot{\rho}_{\text{b}} + 3\frac{\dot{a}}{a}\rho_{\text{b}} + \nabla_i(\rho_{\text{b}}V_{\text{b}}^i) = 0, \quad (6)$$

$$\dot{V}_{\text{b}}^i + \frac{\dot{a}}{a}V_{\text{b}}^i + V_{\text{b}}^j\nabla_jV_{\text{b}}^i + \frac{1}{\rho_{\text{b}}}\nabla^iP + \nabla^i\Psi = \frac{a}{a_0}\frac{n_e\sigma_T}{R}(V_{\gamma}^i - V_{\text{b}}^i), \quad (7)$$

where ρ_{b} and V_{b}^i are the density and the velocity of the baryon-electron fluid, respectively, P is the pressure, σ_T is the Thomson cross section, V_{γ}^i is the dipole moment of the photon field, and R is defined as $R \equiv 3\rho_{\text{b}}/4\bar{\rho}_{\gamma}$ with the spatially averaged energy density of the photon field $\bar{\rho}_{\gamma}$, where $\bar{\quad}$ denotes the background quantity. The right hand side of equation (7) represents the radiation drag force caused through the Compton interaction between electrons and photons which can be written by using τ_{D} that is the time scale of momentum transfer between the baryon-electron fluid and the photon fluid as

$$\frac{a}{a_0}\frac{4\sigma_T\bar{\rho}_{\gamma}x_e}{3m_p}\left(1 - \frac{y_p}{2}\right)(V_{\gamma}^i - V_{\text{b}}^i) \equiv \frac{1}{\tau_{\text{D}}}(V_{\gamma}^i - V_{\text{b}}^i), \quad (8)$$

where m_p denotes the proton mass. As the universe expands, the momentum transfer time scale τ_{D} becomes longer. However the drag time scale is still small enough to keep the tight coupling between baryon-electron and photon fluids even just before the recombination epoch, so that $V_{\gamma}^i = V_{\text{b}}^i$. Eventually the tight coupling breaks down as the recombination process proceeds when the photon mean free path becomes larger than the wavelength of the density perturbations (see also Paper II).

Let us now focus on perturbations of the baryon-electron fluid on very small scales. As far as considering linear density perturbations, perturbations of each scale evolve individually. Following Shaviv (1998), however, we take into account the quasi-nonlinear contribution of the drag force from the large scale velocity field. To be specific, we separate the velocity field into the small scale part which we focus on and the large scale part which describes the nonlinear contribution to the

small scale perturbations as,

$$V_\gamma^i - V_b^i = V_{\gamma(S)}^i - V_{b(S)}^i + V_{\gamma(L)}^i - V_{b(L)}^i, \quad (9)$$

where indices (S) and (L) indicate small and large scales, respectively. The fluctuation of the fractional ionization on the small scale is defined as $\delta x_{e(S)} \equiv x_e - \bar{x}_e$. Then the right hand side of equation (7) leads to

$$\frac{a}{a_0} \frac{4\sigma_T \bar{\rho}_\gamma}{3m_p} \left(1 - \frac{y_p}{2}\right) \left(\bar{x}_e (V_{\gamma(S)}^i - V_{b(S)}^i) + \delta x_{e(S)} \Delta V_0^i\right), \quad (10)$$

where

$$\Delta V_0^i \equiv V_{\gamma(L)}^i - V_{b(L)}^i. \quad (11)$$

Here we ignore higher order terms of the small scale perturbations. The term $\delta x_{e(S)} \Delta V_0^i$ in equation (10) describes the quasi-nonlinear coupling between the large scale shear velocity and the small scale baryon density fluctuations. Adding this quasi-nonlinear term, we can write the linear perturbation equations on the small scale as

$$\dot{\delta}_{b(S)} + \nabla_i V_{b(S)}^i = 0, \quad (12)$$

$$\dot{V}_{b(S)}^i + \frac{\dot{a}}{a} V_{b(S)}^i + c_s^2 \nabla_i \delta_{b(S)} + \nabla_i \Psi_{(S)} = \frac{a}{a_0} \frac{4\sigma_T \bar{\rho}_\gamma}{3m_p} \left(-\bar{x}_e V_{b(S)}^i + \delta x_{e(S)} \Delta V_0^i\right), \quad (13)$$

where c_s is the sound velocity of the baryon-electron fluid defined by $c_s^2 = \dot{P}/\dot{\rho}_b$. In deriving equation (13), we have assumed the isothermal perturbations for the small scale perturbations, i.e., $V_{\gamma(S)}^i = 0$ since the Silk damping process erases the density perturbation and the dipole moment of the photon field on small scales.

Let us investigate the effect of the quasi-nonlinear term $\delta x_{e(S)} \Delta V_0^i$ on the evolution of perturbations. Before the recombination epoch, $\Delta V_0^i = 0$ due to the tight coupling. However, the tight coupling becomes broken down, i.e., $\Delta V_0^i \neq 0$, as the decoupling process proceeds and the contribution from the quasi-nonlinear term may not be negligible anymore. In fact Shaviv has claimed that this quasi-nonlinear contribution, which represents the spatially fluctuating radiation drag force, causes enormous amplification of baryon density fluctuations during the recombination epoch. Hereafter, we omit the label '(S)', for simplicity. Combining equations (12) and (13), we obtain

$$\ddot{\delta}_b + \frac{\dot{a}}{a} \dot{\delta}_b - c_s^2 \Delta \delta_b - \Delta \Psi = -\frac{1}{\tau_D} \delta_b \left(1 + \frac{\Delta V_0^i \nabla_i \delta x_e}{\bar{x}_e \delta_b}\right), \quad (14)$$

where Δ is the Laplacian.

By assuming the wave form solution, $\delta_b \propto e^{(\omega\eta - i\mathbf{x}\cdot\mathbf{k})}$, where \mathbf{k} is the comoving wave number, we have the dispersion relation

$$\omega^2 + \left(\frac{1}{\tau_H} + \frac{1}{\tau_D}\right)\omega + \left(\frac{1}{\tau_0^2} - \frac{1}{\tau_J^2} - i\frac{1}{\tau_R^2}\right) = 0, \quad (15)$$

where

$$\frac{1}{\tau_{\text{H}}} = \frac{\dot{a}}{a} = 3.2 \times 10^{-18} \sqrt{\Omega_0 h^2} \sqrt{1+z} \text{ s}^{-1}, \quad (16)$$

$$\frac{1}{\tau_{\text{D}}} = \frac{a}{a_0} \frac{4\sigma_T \bar{\rho}_\gamma \bar{x}_e}{3m_p} \left(1 - \frac{y_p}{2}\right) = 7.4 \times 10^{-24} \bar{x}_e (1+z)^3 \text{ s}^{-1}, \quad (17)$$

$$\frac{1}{\tau_{\text{o}}} = c_s k = 1.61 \times 10^{-16} (\Omega_b h^2)^{1/3} \left(\frac{M}{M_\odot}\right)^{-1/3} \sqrt{1+\bar{x}_e} \sqrt{1+z} \text{ s}^{-1}, \quad (18)$$

$$\frac{1}{\tau_{\text{J}}} = \sqrt{4\pi G \left(\frac{a}{a_0}\right)^2 \rho_b} = \sqrt{\frac{3\Omega_b}{2\Omega_0}} \frac{1}{\tau_{\text{H}}}, \quad (19)$$

$$\frac{1}{\tau_{\text{R}}} = \sqrt{\frac{|\alpha| \Delta V_0 k}{\tau_{\text{D}}}} = 4.9 \times 10^{-17} (\bar{x}_e |\alpha| \Delta V_0)^{1/2} (\Omega_b h^2)^{1/6} (1+z)^{3/2} \left(\frac{M}{M_\odot}\right)^{-1/6} \text{ s}^{-1}, \quad (20)$$

with $k \equiv |\mathbf{k}|$ and $\Delta V_0 \equiv \Delta V_0^i \cdot k^i / k$ being the shear velocity from the large scale. Here τ_{H} , τ_{D} , τ_{o} , τ_{J} , and τ_{R} are time scales for the Hubble expansion, the radiation drag, the sound oscillation, the Jeans oscillation, and the quasi-nonlinear radiation force, respectively. The parameter α of equation (20) is defined as

$$\alpha \equiv \frac{\delta x_e}{\bar{x}_e \delta_b}. \quad (21)$$

A nonzero value of α provides the quasi-nonlinear effect. Shaviv obtained α by employing the Saha equation. The validity of this assumption will discuss in §4. The derivation of δx_e is shown in Appendix B. In the above expressions, the baryon mass M is used instead of the comoving wave number k (Paper I), which is defined by

$$M = \frac{4\pi \bar{\rho}_b}{3} \left(\frac{\pi a}{k a_0}\right)^3. \quad (22)$$

It should be noticed that we take into account only the baryon component for the gravitational potential.

Let us now evaluate the growth rate of the growing-mode solution. The solution of the dispersion relation (15) can be written as

$$\omega = \frac{1}{2} \left[-\left(\frac{1}{\tau_{\text{H}}} + \frac{1}{\tau_{\text{D}}}\right) + \sqrt{\left(\frac{1}{\tau_{\text{H}}} + \frac{1}{\tau_{\text{D}}}\right)^2 - 4\left(\frac{1}{\tau_{\text{o}}^2} - \frac{1}{\tau_{\text{J}}^2} - i\frac{1}{\tau_{\text{R}}^2}\right)} \right]. \quad (23)$$

Here we omit the negative solution which provides the decaying mode solution. The positive real part of ω , i.e., $\Re[\omega(\eta)]$, represents the growth rate of the instability. The exact expression of $\Re[\omega(\eta)]$ is shown in Appendix A. In the time interval between η_1 and η_2 , the amplification of the baryon density fluctuations, which we refer the growth factor $D(\eta_2, \eta_1)$, becomes

$$D(\eta_2, \eta_1) \equiv \frac{\delta_b(\eta_2)}{\delta_b(\eta_1)} = \exp\left(\int_{\eta_1}^{\eta_2} d\eta \Re[\omega(\eta)]\right). \quad (24)$$

3. Nonlinear Growth of a Toy Model

Before carrying out fully consistent calculations based on density perturbations of actual cosmological models, we investigate the nonlinear growth for a toy model. First, we assume the large scale velocity ΔV_0 is constant in time throughout this section. Secondly, as Shaviv has done in his paper, the fractional ionization \bar{x}_e and its perturbation δx_e are calculated by employing the Saha equation, which is described in Appendix B. We take the fiducial CDM model, i.e., $\Omega_0 = 1.0$, $\Omega_b = 0.04$, and $h = 0.5$. The time evolution of the fractional ionization is shown in Fig. 1. We also plot the redshift visibility function

$$g(z) \equiv -\frac{d\tau}{dz} e^{-\tau}, \quad (25)$$

where $\tau \equiv -\int_{\eta}^{\eta_0} d\eta' \frac{a}{a_0} n_e \sigma_T$ is the optical depth. The width of the visibility function corresponds to the recombination epoch. Therefore the recombination epoch of this model is $1+z = 1500 - 1100$.

Let us first compare time scales of equations (16)–(20). In Fig. 2, these (inverse) time scales are plotted as a function of $(1+z)$. The panel (a) shows $1/\tau_D$, $1/\tau_H$, and $1/\tau_J$, all which do not depend on k . Note that $1/\tau_D$ dominates others before and during the recombination epoch. However as the recombination process proceeds, this time scale suddenly increases and eventually exceeds other time scales after recombination. In this panel, we plot τ_o/τ_R^2 which is also independent on k . We will discuss this variable later in this section.

In the panel (b), we plot $1/\tau_o$ and $1/\tau_R$ for different wave numbers k , i.e., $k = 71.2, 330, 1530, 7120$, and 33000Mpc^{-1} which correspond to mass scales $10^6, 10^4, 10^2, 10^0$, and $10^{-2} M_\odot$, respectively.

Now let us discuss the growth rate $\Re[\omega(\eta)]$ by comparing the time scales in the expression (23). As is shown in Fig. 2, the larger the wave number k , the larger the inverse time scales $1/\tau_R$ and $1/\tau_o$ become. Therefore we expect to obtain the maximum growth rate when we take the small scale limit, i.e., $k \rightarrow \infty$. As is shown in Appendix A, the real part of the square root term of equation (23) approaches to τ_o/τ_R^2 which is the combination seen in the panel (a) of Fig. 2. Shaviv claimed that this combination provides the maximum growth rate, i.e.,

$$\Re[\omega(\eta)]_{\text{max}}^{\text{Shav}} = \frac{\tau_o}{2\tau_R^2} = \frac{\alpha\Delta V_0}{2c_s\tau_D}. \quad (26)$$

However, this is not the whole story. The complete expression of equation (23) with large k limit becomes

$$\Re[\omega(\eta)]_{\text{max}} \equiv \lim_{k \rightarrow \infty} \Re[\omega] = -\frac{1}{2} \frac{1}{\tau_D} + \frac{\tau_o}{2\tau_R^2} = -\frac{1}{2} \frac{1}{\tau_D} + \frac{\alpha\Delta V_0}{2c_s\tau_D}. \quad (27)$$

Here we ignore the inverse Hubble time scale because it is much smaller than $1/\tau_D$ during recombination. Remember that $1/\tau_D$ is comparable to τ_o/τ_R^2 during recombination as is shown in Fig. 2(a). In fact, the existence of this $1/\tau_D$ term suppresses the nonlinear growth a lot. From

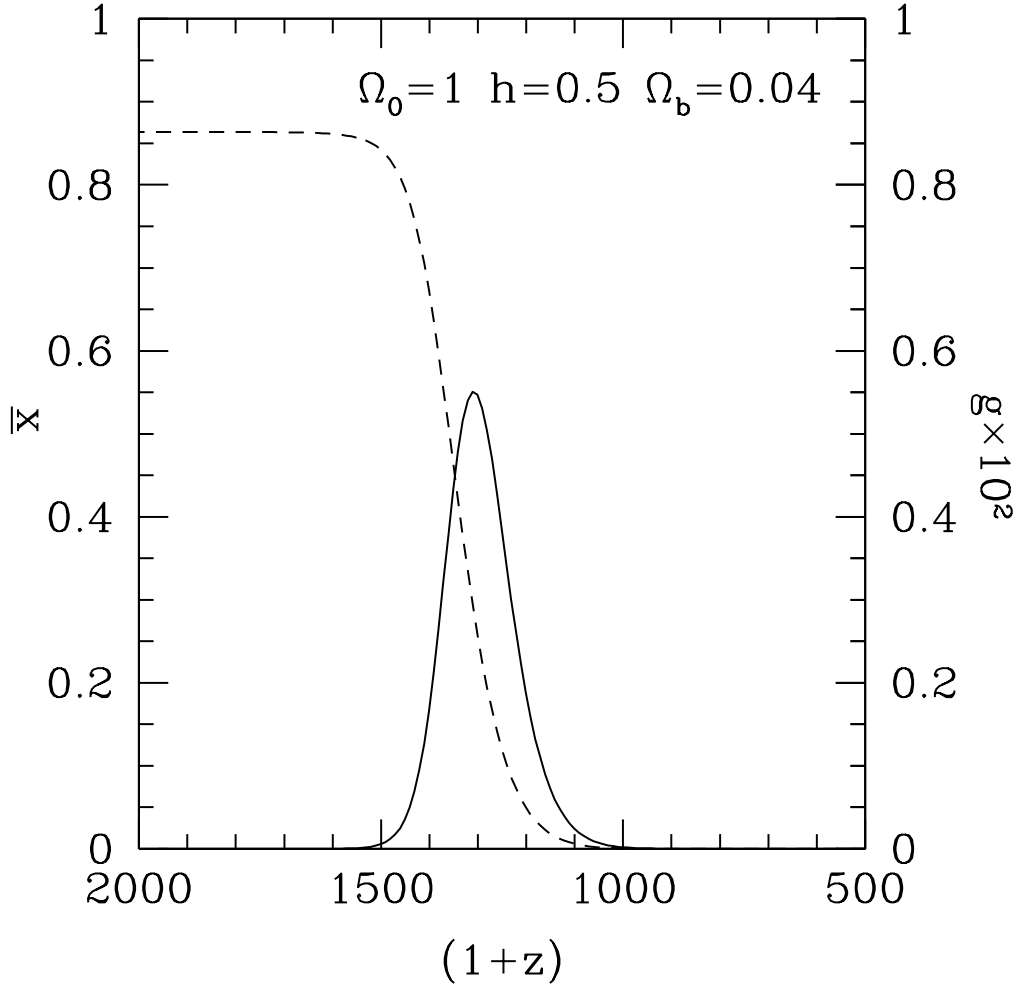


Fig. 1.— Fractional ionization \bar{x}_e (dashed line) and visibility function $g(z)$ (solid line) from the Saha equation with the CDM model; $\Omega_0 = 1.0$, $\Omega_b = 0.04$, and $h = 0.5$. The peak of the visibility function ($z = 1300$) corresponds to the recombination epoch. In this fiducial CDM model, the recombination occurs in between $1 + z = 1500$ and 1100 .

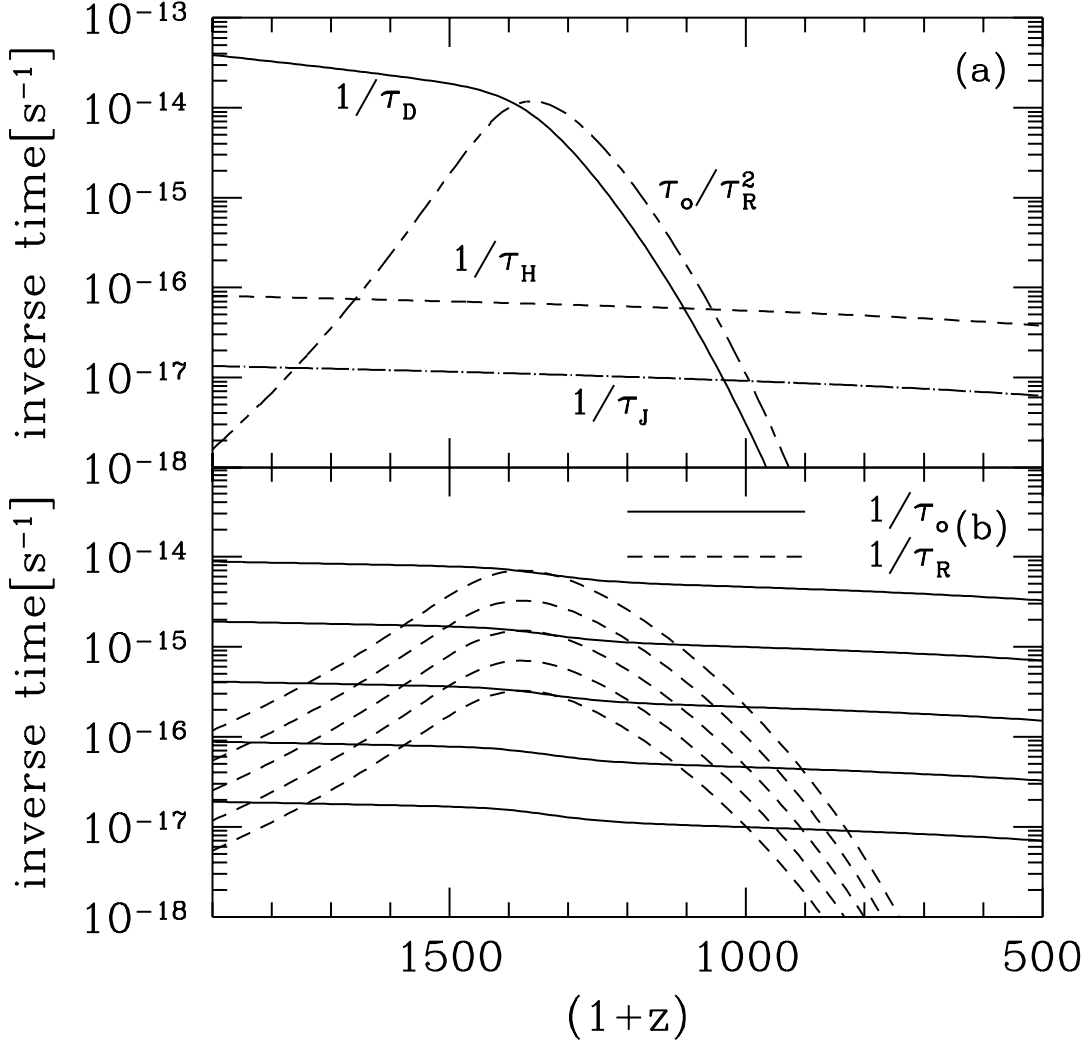


Fig. 2.— Inverse time scales (eq. [16] - eq. [20]) for the fiducial CDM model as in Fig. 1. The Saha equation is employed to calculate the fractional ionization and $\Delta V_0 = 10^{-4}$ for τ_R . Wave number independent and dependent time scales are plotted in (a) and (b), respectively. In panel (a), τ_o/τ_R^2 which provides the maximum growth rate together with τ_D (eq.[27]) is also plotted by a long dashed-short dashed line. In panel (b), the wave numbers of the baryon density perturbations are $k = 71.2, 330, 1530, 7120,$ and 33000Mpc^{-1} which correspond to mass scales $10^6, 10^4, 10^2, 10^0,$ and $10^{-2} M_\odot$, respectively, from bottom to top.

equation (27), it is found that a sufficient condition for the nonlinear growth at least on the smallest scale is $\Re[\omega(\eta)]_{\max} > 0$, i.e.,

$$\alpha\Delta V_0 > c_s. \quad (28)$$

In Fig. 3, the growth rates and the growth factors of the toy model are plotted for various wave numbers and the large wave number limit.

From this figure, it is found that the growth rate and the growth factor are very sensitive to the value of the large scale velocity field ΔV_0 . The growth factor of $\Delta V_0 = 10^{-4}$ is more than factor 20 larger than the one of $\Delta V_0 = 6 \times 10^{-5}$ for the large k limit.

The “maximum” growth rates and growth factors obtained by Shaviv’s formula (eq. [26]) are also plotted for comparison in Fig. 3. It is clear that neglect of the diffusion results in the extremely large false growth factor. By the correct treatment, rather mild growth is found. When we take relatively large velocity $\Delta V_0 = 10^{-4}$, we obtain about factor 50 growth factor while Shaviv’s treatment induces more than 10^5 growth of small scale density perturbations. From Fig. 3, it is shown that the nonlinear growth mechanism starts to work in the relatively early epoch ($z \sim 1500$) if we neglect the diffusion term. However, by the correct treatment, it is found that the nonlinear growth works only when $\tau_o/\tau_R^2 > 1/\tau_D$, i.e., $1 + z < 1340$ in this fiducial CDM model as is shown in Fig. 2. Even in this shorter period, the maximum growth rate is suppressed by the existence of the diffusion term (eq. [27]). We should conclude that the enormous growth $\sim 10^4$ of the baryon density fluctuations which Shaviv claimed in his paper is not likely to happen.

However, we should emphasize that this nonlinear growth mechanism still works and enhances the baryon density perturbations. It is interesting to estimate the nonlinear growth factor for realistic cosmological models.

4. Nonlinear Growth in adiabatic CDM Models

Since it is generally believed that adiabatic small scale baryon density perturbations decay out before and during the recombination epoch due to the diffusion (Silk) damping, an additional assumption to standard adiabatic perturbations seems to be needed for the nonlinear growth mechanism which requires the existence of small scale baryon perturbations. In the paper by Shaviv (1998), for example, he artificially assumed the existence of baryon isothermal density perturbations.

However, we should point out that small scale *isothermal* baryon density perturbations are in fact existing at the recombination epoch in *general adiabatic* CDM models. Recently, the authors of the present paper (K.Y. & N.S.) and Sato have found that small scale baryon perturbations grow after the diffusion (Silk) damping even before the recombination epoch (Paper II). This growth of baryon density perturbations before the recombination epoch is the result of the breaking of the tight-coupling between the baryon perturbations and the photon perturbations

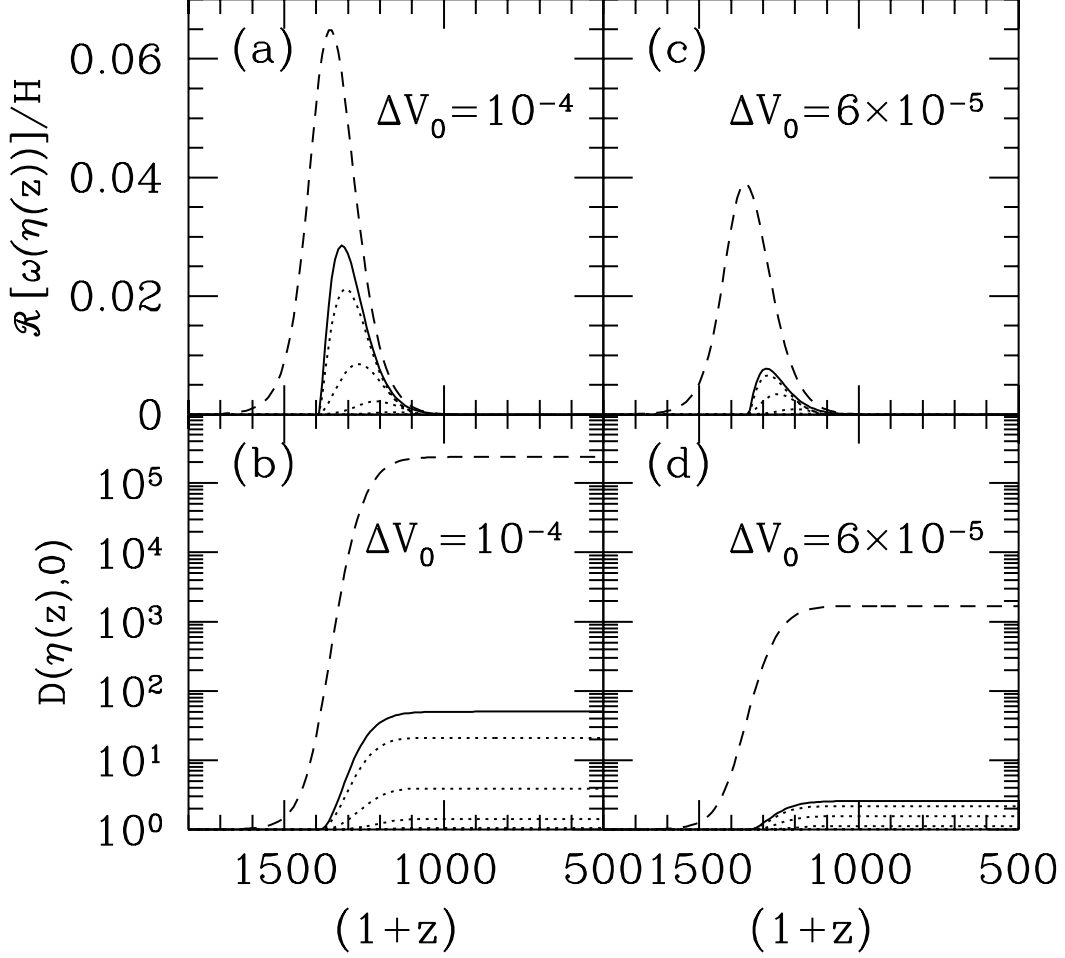


Fig. 3.— Growth rates $\mathfrak{R}[\omega(\eta(z))]$ ((a) and (c)) in the unit of the Hubble time and growth factors $D(\eta(z), 0) \equiv \exp(\int_0^\eta d\eta' \mathfrak{R}[\omega(\eta')]) = \exp(\int_{1+z}^\infty d(1+z') \mathfrak{R}[\omega]/H)$ ((b) and (d)) of two simple simulations with fixed shear velocities $\Delta V_0 = 10^{-4}$ and 6×10^{-5} for the same model as in Fig. 1. The dotted lines plot the growth rates or growth factors for the wave numbers $k = 33000, 7120, 1530, 330,$ and 71.2Mpc^{-1} from top to bottom. One can see almost no growth for $k = 330$ and 71.2Mpc^{-1} . The solid lines are the maximum growth rates (eq. [27]) and growth factors. The maximum growth rates and growth factors of the investigation by Shaviv (eq. [26]) are also plotted by dashed lines for comparison. It is shown that inclusion of the diffusion term $1/\tau_D$ (eq. [27]) results in the significant suppression of the growth factors.

on small scales. The growth is characterized by the terminal velocity, which implies the balance between the gravitational force due to the potential of CDM and the friction force by the Compton interaction with background photons. According to the previous investigation in Paper II, the Fourier coefficient of the small scale baryon perturbations grows in proportion to $(1+z)^{-7/2}$. The small scale baryon density perturbations have amplitude of order $\mathcal{O}(10^{-2}) \sim \mathcal{O}(10^{-3})$ compared with the CDM perturbations.

The small scale photon perturbations are smeared out by the diffusion damping. On the other hand, the energy transfer between the baryon-electron fluid and the background photons is effective during and for some time after the recombination epoch. Therefore the nature of the small scale baryon perturbations is isothermal during these epochs (see Paper I). These isothermal baryon perturbations could be enhanced by the nonlinear growth mechanism although the growth factor may not be as large as originally thought by Shaviv as is described in the previous section.

The amplitude of the large scale velocity field ΔV_0 is crucial for the instability as is shown in Fig. 3. In linear theory of density perturbations, the variance of square of the large scale velocity field is evaluated by

$$\langle |V_\gamma^i - V_b^i|^2 \rangle = \frac{1}{2\pi^2} \int dk k^2 |V_\gamma(k, \eta)^i - V_b(k, \eta)^i|^2, \quad (29)$$

where $V_\gamma(k, \eta)^i$ and $V_b(k, \eta)^i$ are Fourier coefficients of the dipole anisotropy of the photon field and the peculiar velocity field of the baryon fluid, respectively. Introducing the parameter ν , we derive the large scale velocity field from the rms one as

$$\Delta V_0 = \nu \sqrt{\langle |V_\gamma^i - V_b^i|^2 \rangle}. \quad (30)$$

We consistently solve the linear perturbations of the photon, baryon, and dark matter system in the expanding universe to calculate the rms velocity on large scales. In Fig. 4, the rms velocities of various COBE normalized CDM models are shown. It is found that the rms velocities are typically 10^{-6} just before recombination. They rapidly increase toward 10^{-4} as the recombination process proceeds when the tight coupling between photons and baryons breaks. We may conclude that effective values of the rms velocities during the recombination epoch are about a few times 10^{-5} regardless of model parameters. According to our toy model calculations as is shown in Fig. 3, therefore, we expect only high velocity peaks induce the nonlinear growth on small scales in the realistic cosmological models.

To calculate the growth rate and the growth factor of baryon density fluctuations, we need to obtain perturbations of the fractional ionization δx_e . Once we can get δx_e , we calculate α , which is defined by equation (21) to estimate τ_R . Using baryon density fluctuations δ_b of the previous time step, we can calculate τ_R , the growth rate and the growth factor. We can estimate δ_b with multiplying this growth factor by the amplitude of linear density perturbations with the COBE normalization.

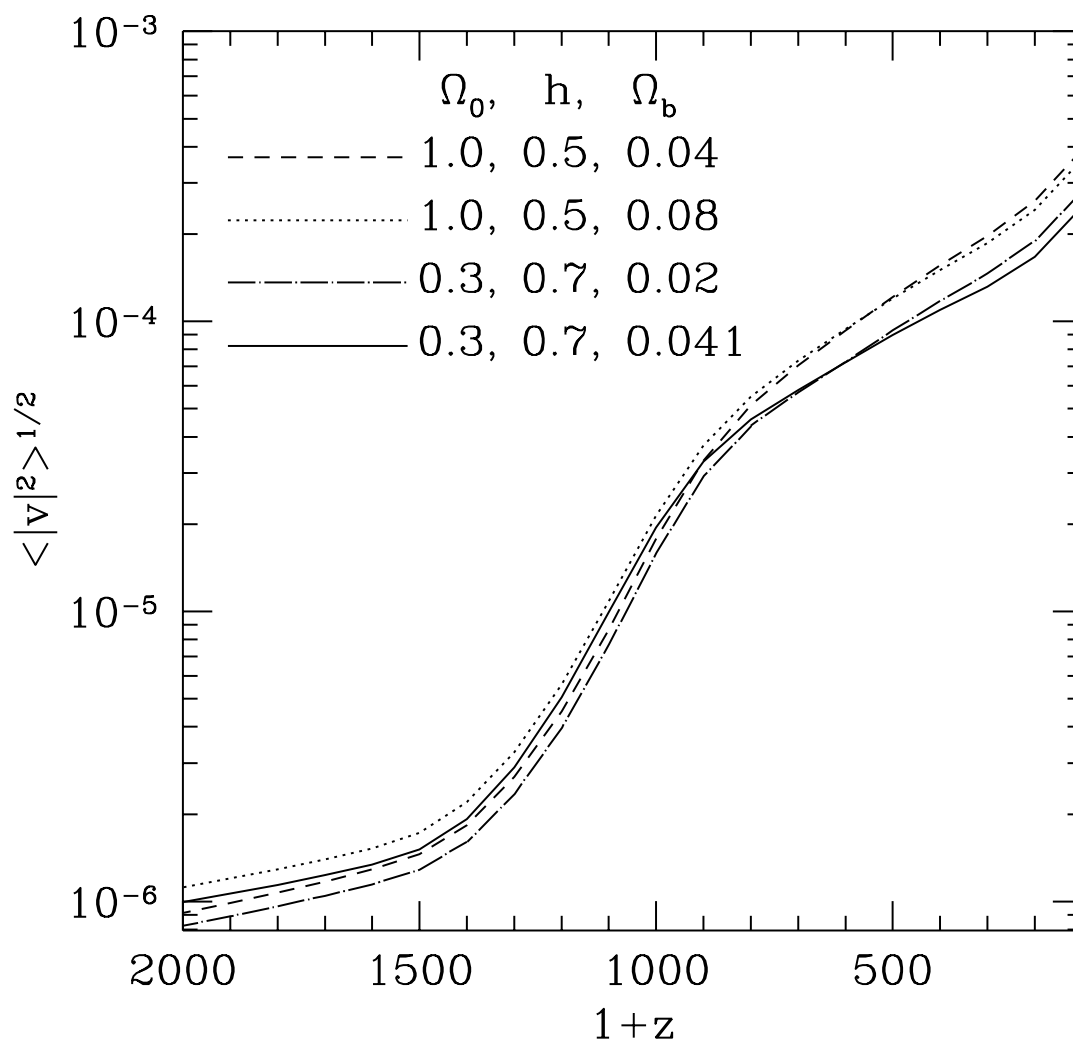


Fig. 4.— Root mean square shear velocities in large scales. The COBE normalized velocities of various flat CDM models grow typically from 10^{-6} to 7×10^{-5} during the recombination epoch.

Strictly speaking, we may have to solve radiative transfer during the recombination epoch to get precise value of fluctuations of δx_e . Instead, we have employed two approximation methods here.

First method is to employ Saha’s formula as Shaviv has done in his paper, which is a very simple but unrealistic assumption during and after the recombination epoch. It is well known that even the fractional ionization itself leaves from the value by Saha’s formula as recombination proceeds (see e.g., Jones & Wise 1985). Therefore we next develop a perturbed treatment of the rate equation. Detailed treatments of these two methods are described in Appendix B. It is shown there that these two methods provide very different \bar{x}_e and δx_e .

It is found that the nonlinear growth mechanism does not work at all for the fiducial CDM model with $\Omega_0 = 1, \Omega_b = 0.04$, and $h = 0.5$ if we employ the Saha equation for the evolution of \bar{x}_e and δx_e . It is because ΔV_0 is too small during the recombination epoch, i.e., $1 + z = 1500$ and 1100 . In this calculation, $1/\tau_H + 1/\tau_D > \tau_o/\tau_R^2$ for all time, which leads to the real part of ω of equation (23) to be negative on small scales.

If we employ the perturbed rate equation to calculate δx_e , however, the nonlinear growth mechanism is effective since the recombination process continues until much later epoch, $z \sim 800$ as is shown in Fig. 7 in Appendix B, when ΔV_0 is large enough to induce the nonlinear growth by the drag force. We obtain the nonlinear growth factor as a function of redshift z in Fig. 5 for various COBE normalized CDM models, i.e., the fiducial model with $\Omega_0 = 1$ and $h = 0.5$ and low density flat and open models with $\Omega_0 = 0.3$ and $h = 0.7$. For the purpose of comparison, different values of baryon density, i.e., $\Omega_b h^2 = 0.01$ and $\Omega_b h^2 = 0.02$ are considered. We adopt $3 - \sigma$ peaks for the amplitude of the large scale velocity field. The nonlinear growth mechanism works from $z = 1100$ to $z = 800 \sim 600$ which depends on the value of $\Omega_b h^2$.

Fig. 6 plots the final growth factors as a function of wave number k . We find that the growth factors of low density CDM models are less than the ones of $\Omega_0 = 1$ models. It is mostly because the COBE normalized rms velocity fields of low density models are smaller when the mechanism effectively works ($z = 1100 \sim 800$) as is shown in Fig. 4. The strong Ω_b dependence of the growth factor is also found in Fig. 6. The reason is following. The residual ionization at low redshifts scales as $\bar{x}_e \propto \Omega_0^{1/2}/(\Omega_b h)$ (see e.g., Peebles 1993). Therefore we have smaller \bar{x}_e for larger Ω_b . The maximum growth rate can be written as (eq. [27]), $\Re[\omega(\eta)]_{\max} = (\alpha \Delta V_0 / 2c_s - 1) / (2\tau_D)$. As is shown in Fig. 8 in Appendix B, the Ω_b dependence of α is relatively weak because of cancellation in between \bar{x}_e and δx_e . The remaining dependence appears through $1/\tau_D \propto \bar{x}_e$. For larger Ω_b , therefore, \bar{x}_e and the maximum growth factor become smaller.

5. Summary

We investigate the evolution of the baryon density perturbations on very small scales, especially focus on the nonlinear growth induced by the shear velocity field on large scales, which

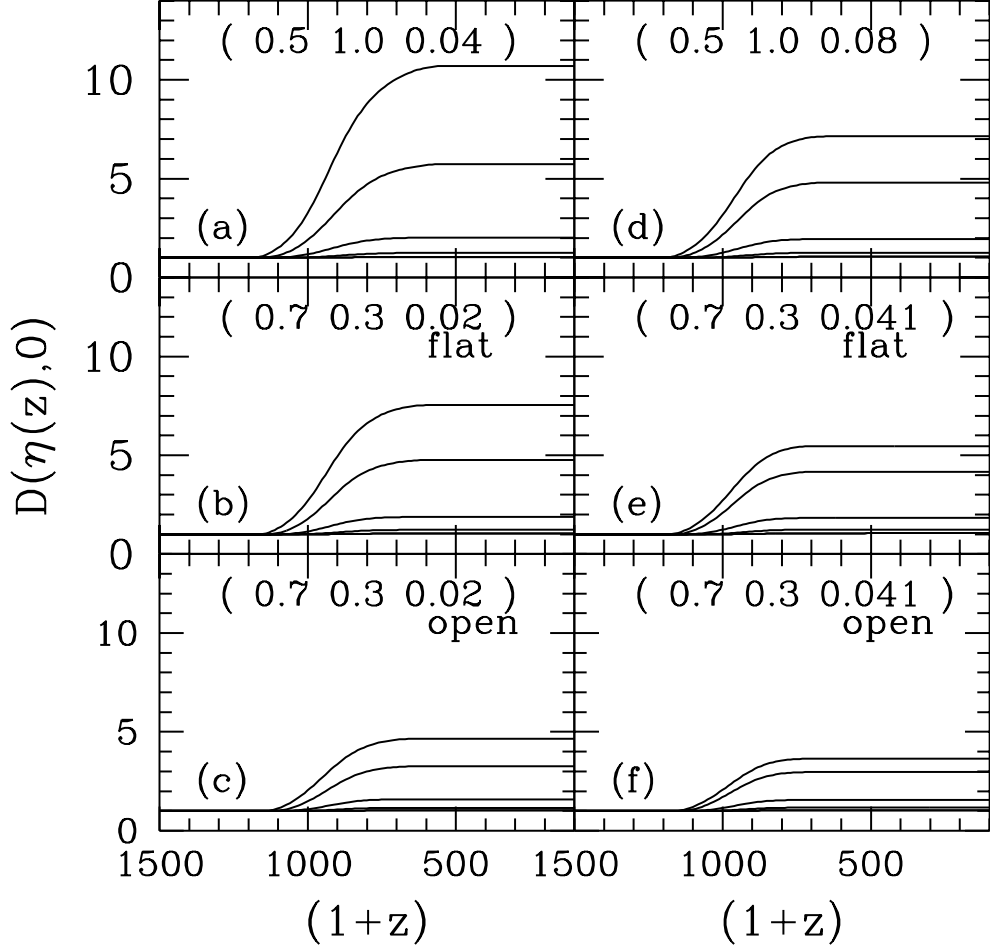


Fig. 5.— Growth factor $D(\eta(z), 0) \equiv \exp\left(\int_0^\eta d\eta' \Re[\omega(\eta')]\right)$ for various CDM models. The large scale velocity field ΔV_0 is consistently solved by linear density perturbations with COBE normalization (see Fig. 4). The $3 - \sigma$ velocity peaks ($\nu = 3$) are considered. The fractional ionization and its fluctuation are computed by the rate equation. In parentheses, the cosmological parameters h , Ω_0 , and Ω_b are shown. The mass scales of the baryon perturbations are 10^{-2} , 10^0 , 10^2 , 10^4 , and $10^6 M_\odot$ from top to bottom, respectively. Panel (b) and (e) are low density flat models while (c) and (f) are open models.

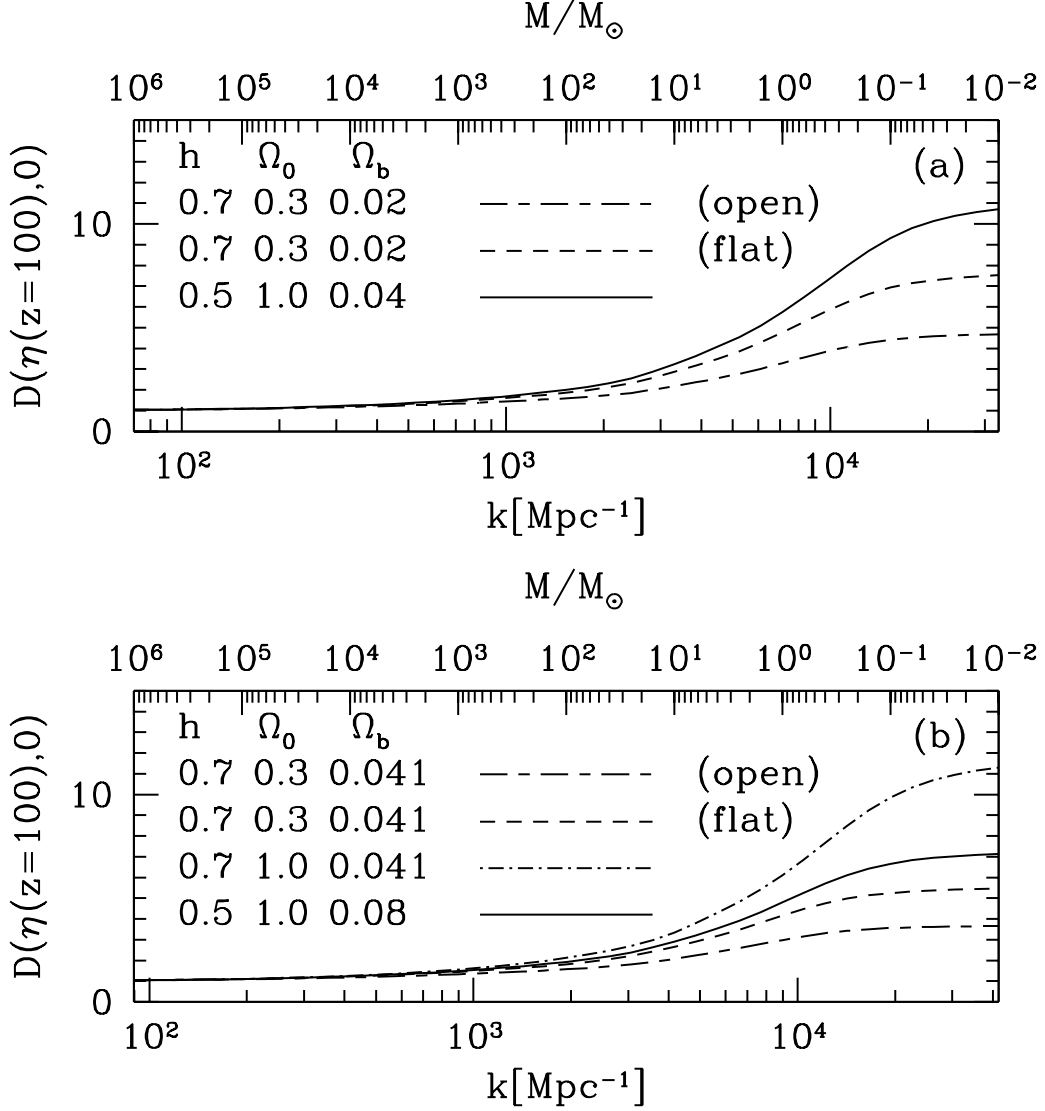


Fig. 6.— Final growth factor $D(\eta(z = 100), 0)$ for various cosmological models with $\nu = 3$ as a function of the wave number. The growth factor of the smallest baryon perturbation scale we chose ($M = 10^{-2}M_\odot$) is close to the maximum growth factor $\exp\left(\int d\eta \Re[\omega(\eta)]_{\max}\right)$, where $\Re[\omega(\eta)]_{\max}$ is defined in equation (27).

is originally proposed by Shaviv (1998).

First we study this nonlinear evolution with employing simple assumptions, i.e., the constant large scale shear velocity field and the Saha equation for the calculations of the fractional ionization and its fluctuation. What we find is not enormous amplification of density fluctuations but relatively mild growth. The reason of Shaviv’s overestimation is because he has neglected the diffusion term which suppresses the growth.

It is found that the growth factor is very sensitive to the value of the large scale shear velocity field. Only small difference ($\Delta V_0 = 10^{-4}$ versus 6×10^{-5}) causes huge divergence of the final growth factor (factor 50 versus 2.5).

Following the previous works (Paper I & II), we next apply the nonlinear growth mechanism to density perturbations of general adiabatic CDM models. In these works, it has been found that the baryon density perturbations are not completely erased by diffusion damping if there exists gravitational potential of CDM. They even grow before recombination under the balance between the radiative drag force and the gravitational force. We investigate the nonlinear growth of these baryon density fluctuations with employing the perturbed rate equation which is proposed first time in this paper. The results are followings: (1) The nonlinear growth is larger in smaller scales. This mechanism only affects the perturbations whose scales are smaller than $10^2 M_\odot$. (2) The maximum growth factors of baryon density fluctuations by this mechanism for various COBE normalized CDM models are typically less than factor 10 even if we take $3 - \sigma$ large scale velocity peaks. (3) The strong Ω_b dependence of the growth factor is found. This is because of the Ω_b dependence of the residual ionization. The fractional ionization \bar{x}_e , which is proportional to the inverse diffusion time scale and the maximum growth rate, is larger for smaller Ω_b .

How could this nonlinear growth mechanism affect on the structure formation in the high redshift universe? It is very interesting coincidence that the typical scale of the nonlinear growth is about the stellar size ($\lesssim 10^2 M_\odot$). However we need to carry out high resolution numerical simulations to investigate the evolution of the stellar scale density fluctuations on which a lot of other complicated physical processes, i.e., shock heating, UV radiation from first stars or AGN, cooling and so on, work. Our quasi-linear perturbation analysis provides the initial condition for the calculations of such complicated structure formation in the high-z universe. The transfer function of the baryon density perturbations can be obtained by multiplying the nonlinear growth factor by the transfer function of the linear perturbations which is derived in Paper II.

ACKNOWLEDGEMENT

We thank Dr. Tsuribe for stimulating discussions. We also thank Professors Sato and Kojima for comments. The authors (K.Y. and H.N.) are grateful to Y. Kadoya for discussions related to the topics of the present paper. This research was supported by the Inamori Foundation, Sumitomo

Foundation, and in part by the Grants-in-Aid program (11640280 & 11640235) by the Ministry of Education, Science, Sports and Culture of Japan. G.L. gratefully acknowledges the fellowship of Interchange Association.

A. Real Part of the Complex Square Root

The derivation of the positive real part of the complex square root term in equation (15) is shown in this appendix. In general, the square root of an arbitrary complex number can be rewritten as

$$\sqrt{A + Bi} = \sqrt{\sqrt{A^2 + B^2}(\cos \alpha + i \sin \alpha)} = \sqrt{\sqrt{A^2 + B^2}} \exp\left(\frac{i\alpha}{2}\right), \quad (\text{A1})$$

where A and B are real numbers and

$$\cos \alpha = \frac{A}{\sqrt{A^2 + B^2}}, \quad \sin \alpha = \frac{B}{\sqrt{A^2 + B^2}}. \quad (\text{A2})$$

Hence the real part of this square root is

$$\begin{aligned} \Re[\sqrt{A + Bi}] &= \sqrt{\sqrt{A^2 + B^2}} \cos \alpha/2 \\ &= \sqrt{\frac{1}{2} \left(A + \sqrt{A^2 + B^2} \right)}. \end{aligned} \quad (\text{A3})$$

Let us now take

$$A = \left(\frac{1}{\tau_{\text{H}}} + \frac{1}{\tau_{\text{D}}} \right)^2 + 4 \frac{1}{\tau_{\text{J}}^2} - 4 \frac{1}{\tau_{\text{O}}^2}, \quad (\text{A4})$$

$$B = 4 \frac{1}{\tau_{\text{R}}^2}. \quad (\text{A5})$$

In the small scale limit, i.e., $k \rightarrow \infty$, we have $1/\tau_{\text{O}}^2 \gg 1/\tau_{\text{R}}^2 \gg 1/\tau_{\text{D}}^2$, so that $|A| \gg B$. We have to keep in mind that A is negative in this limit. Accordingly, we obtain the following approximation:

$$\Re[\sqrt{A + Bi}] = \sqrt{\frac{1}{2}|A| \left(-1 + \sqrt{1 + B^2/A^2} \right)} \simeq \frac{B}{2\sqrt{|A|}} \simeq \frac{\tau_{\text{O}}}{\tau_{\text{R}}^2}. \quad (\text{A6})$$

B. Saha versus Rate Equations

Some aspects of the baryon-electron system dealt with the recombination rate have been discussed in the previous papers (Paper I, II). In Paper I, the perturbed rate equation for hydrogen has been presented, while the helium fraction has been neglected and the time-evolution of the equation has not been solved. In the present paper we derive a new formula for the perturbation

of the fractional ionization taking the helium fraction into account. The evolution of the fractional ionization x_e is described as (Peebles, 1968)

$$-\frac{d}{dt}x_e = r_e n_b \left(1 - \frac{y_p}{2}\right) \left\{ x_e^2 - \left[1 - y_p - \left(1 - \frac{y_p}{2}\right)x_e\right] \frac{x_s^2}{1 - y_p - (1 - y_p/2)x_s} \right\} C, \quad (\text{B1})$$

where r_e is the recombination coefficient, x_s is the fractional ionization derived in use of the Saha equation and C is the suppression factor. We employ the fitting formula for the recombination coefficient by Pequignot et al. (1991) as

$$r_e = 10^{-13} \frac{aT_4^b}{1 + cT_4^d} \text{cm}^3 \text{s}^{-1}, \quad (\text{B2})$$

where the fitting constants are $a = 4.309$, $b = -0.6166$, $c = 0.6703$, and $d = 0.5300$, and T_4 is the baryon temperature in the unit of $10^4 K$, i.e., $T_4 \equiv T_b/10^4 K$. From the Saha equation, x_s can be derived as

$$\frac{(1 - y_p/2)^2 x_s^2}{1 - y_p - (1 - y_p/2)x_s} = \frac{(2\pi m_e T)^{3/2}}{n_b (2\pi)^3} e^{-13.6\text{eV}/T}. \quad (\text{B3})$$

The suppression factor C in the right hand side is

$$C = \frac{1 + K\Lambda n_{1s}}{1 + K(\Lambda + \beta_e)n_{1s}}, \quad (\text{B4})$$

where n_{1s} is the number density of hydrogen in the electron state, Λ is the two-photon decay rate from the excited state to the ground state, $\beta_e = r_e(m_e T/2\pi)^{3/2} e^{-3.4\text{eV}/T}$ and $K = (a/\dot{a})\lambda_\alpha^3/8\pi$ with λ_α being the Lyman alpha photon wave length.

Let us derive the perturbation equations on very small scales. We introduce the perturbed variables,

$$x_e = \bar{x}_e(\eta) + \delta x_e(\eta, \mathbf{x}), \quad (\text{B5})$$

$$x_s = \bar{x}_s(\eta) + \delta x_s(\eta, \mathbf{x}), \quad (\text{B6})$$

$$n_b = \bar{n}_b(\eta)(1 + \delta_b(\eta, \mathbf{x})), \quad (\text{B7})$$

where $\bar{}$ denotes the background quantities. We ignore the temperature perturbation δT since we are only interested in perturbations on very small scales where δT is erased by Silk damping.

The unperturbed quantities $\bar{x}_e(\eta)$ and $\bar{x}_s(\eta)$ satisfy the same equations as (B1) and (B3) with replaced n_b , x_e , and x_s by \bar{n}_b , \bar{x}_e , and \bar{x}_s , respectively. Then, from the Saha equation (B3), we find the linear perturbation equation for δx_s as,

$$\delta x_s = -\frac{1 - y_p - (1 - y_p/2)\bar{x}_s}{2(1 - y_p) - (1 - y_p/2)\bar{x}_s} \bar{x}_s \delta_b. \quad (\text{B8})$$

No perturbation of the fractional ionization can be generated before recombination since $\bar{x}_s = (1 - y_p)/(1 - y_p/2)$.

From equation (B1), on the other hand, we can obtain the linear perturbation equation for δx_e as,

$$-\frac{d}{dt}\delta x_e = Cr_e\bar{n}_b(1-y_p/2)\left\{\delta_b\bar{x}_e^2 + \delta x_e\left[2\bar{x}_e + \frac{(1-y_p/2)\bar{x}_s^2}{1-y_p-(1-y_p/2)\bar{x}_s}\right]\right. \\ \left.+ \frac{\delta C}{C}\left[\bar{x}_e^2 - [1-y_p-(1-y_p/2)\bar{x}_e]\frac{\bar{x}_s^2}{1-y_p-(1-y_p/2)\bar{x}_s}\right]\right\}, \quad (\text{B9})$$

where

$$\frac{\delta C}{C} = -\frac{K\beta_e\bar{n}_b[(1-y_p-(1-y_p/2)\bar{x}_e)\delta_b - (1-y_p/2)\delta x_e]}{[1+K\Lambda\bar{n}_b(1-y_p-(1-y_p/2)\bar{x}_e)][1+K(\Lambda+\beta_e)\bar{n}_b(1-y_p-(1-y_p/2)\bar{x}_e)]}. \quad (\text{B10})$$

Fig. 7(a) plots the fractional ionization \bar{x}_s and \bar{x}_e for the fiducial CDM model ($\Omega_0 = 1.0$ and $h = 0.5$) and the Λ CDM model ($\Omega_0 = 0.3$ and $h = 0.7$) with high and low baryon densities, i.e., $\Omega_b h^2 = 0.01$ and 0.02 .

The evolution of the Fourier coefficients of δx_s and δx_e are plotted in Fig. 7(b). Here we adopt the COBE normalized baryon density perturbation with the wave number $k = 7120\text{Mpc}^{-1}$ which corresponds to $1M_\odot$. The nonlinear growth is taken into account to calculate the baryon density perturbation. Before recombination, $\bar{x}_e \approx \bar{x}_s$ and $\delta x_e \approx \delta x_s$. As the recombination process proceeds, \bar{x}_s rapidly decreases and δx_s falls as rapid as \bar{x}_s because δx_s is roughly proportional to \bar{x}_s in equation (B8) if $\bar{x}_s \ll 1$. On the other hand, if we employ the rate equation, the recombination process proceeds much slower and eventually there remains the residual ionization as is shown in Fig. 7(a). This residual ionization results in the residual perturbation of the fractional ionization too. Therefore thermal equilibrium is not a good approximation for neither \bar{x} nor δx .

As is discussed in §2, the drag force due to the perturbations of the fractional ionization is parameterized by α/τ_D . Here we define $\alpha_s \equiv \delta x_s/(\bar{x}_s\delta_b)$ and $\alpha_e \equiv \delta x_e/(\bar{x}_e\delta_b)$ to distinguish α 's obtained by the Saha equation and the rate equation, respectively.

One can easily derive α_s from equation (B8) as

$$\alpha_s = -\frac{(1-y_p)-(1-y_p/2)\bar{x}_s}{2(1-y_p)-(1-y_p/2)\bar{x}_s}. \quad (\text{B11})$$

Before the recombination epoch, $\alpha_s = 0$. And $\alpha_s = -1/2$ when the fractional ionization can be neglected. This value $-1/2$ is assumed in Shaviv's calculations. On the other hand, α_e is numerically calculated. Fig. 8 plots α_e and α_s as a function of $(1+z)$ for various cosmological models. It is found that α_e 's are nearly twice as large as α_s 's during recombination when the nonlinear growth mechanism works.

In Fig. 9, we plot $|\alpha|/\tau_D$ for same cosmological models. Since the radiation drag force is proportional to $|\alpha|/\tau_D$, we expect larger amplification of the baryon density perturbations if we employ the rate equation instead of the Saha equation which Shaviv has used. Moreover, the

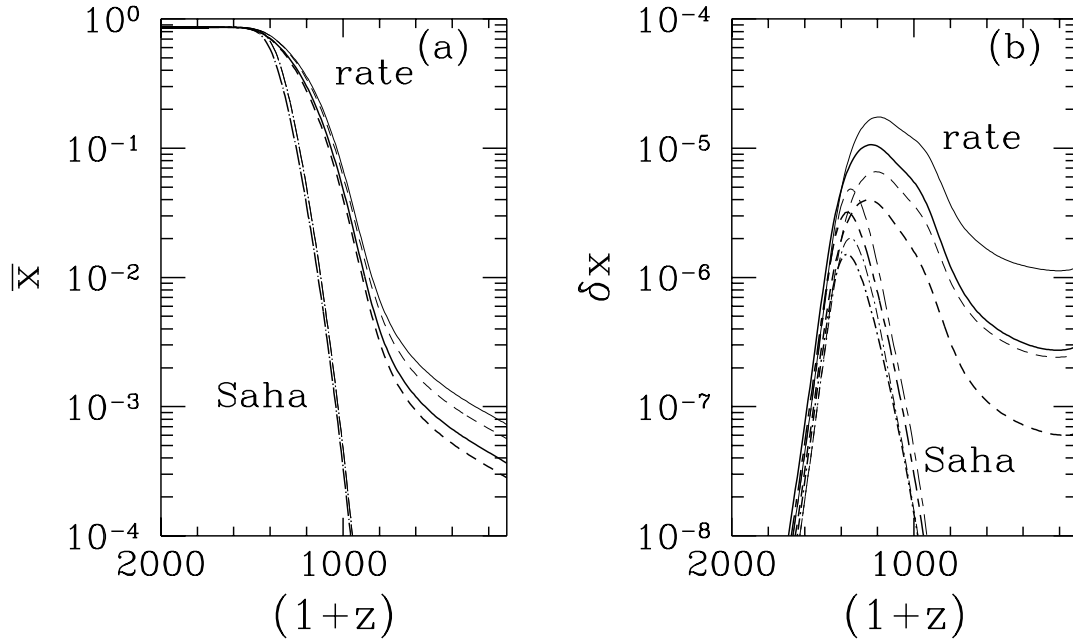


Fig. 7.— Fractional ionization (a) and its perturbation (b) from the Saha equation and the rate equation. We have two values of $\Omega_b h^2$; 0.01 and 0.02 denoted by thin and thick lines, respectively. The solid and dashed lines describe the models with $\Omega_0 = 1.0$ and $h = 0.5$ and $\Omega_0 = 0.3$ and $h = 0.7$, respectively, for the rate equation. In panel (b), long dashed-short dashed lines denote the models with $\Omega_0 = 0.3$ and $h = 0.7$ and dot-dashed lines denote $\Omega_0 = 1.0$ and $h = 0.5$ for the Saha equation. Since the fractional ionization depends only on the value of $\Omega_b h^2$ in the Saha equation (B3), one can find only two lines for \bar{x} with the Saha equation in panel (a). The wave number k is adopted as 7120Mpc^{-1} .

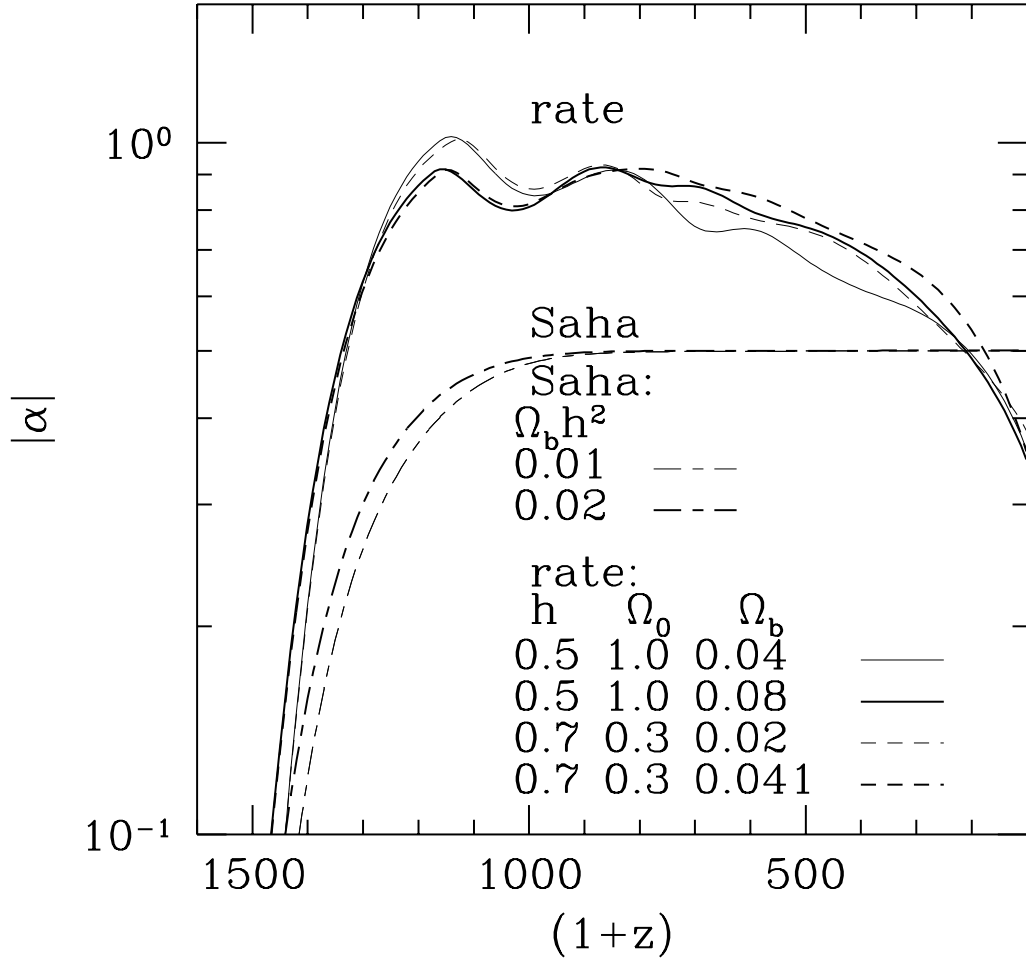


Fig. 8.— Parameter $|\alpha|$ (eq. [21]) from the rate equation and the Saha equation for various cosmological models. When the fractional ionization is small enough, $|\alpha| = 0.5$ in use of the Saha equation. The wave number k is adopted as 7120Mpc^{-1} .

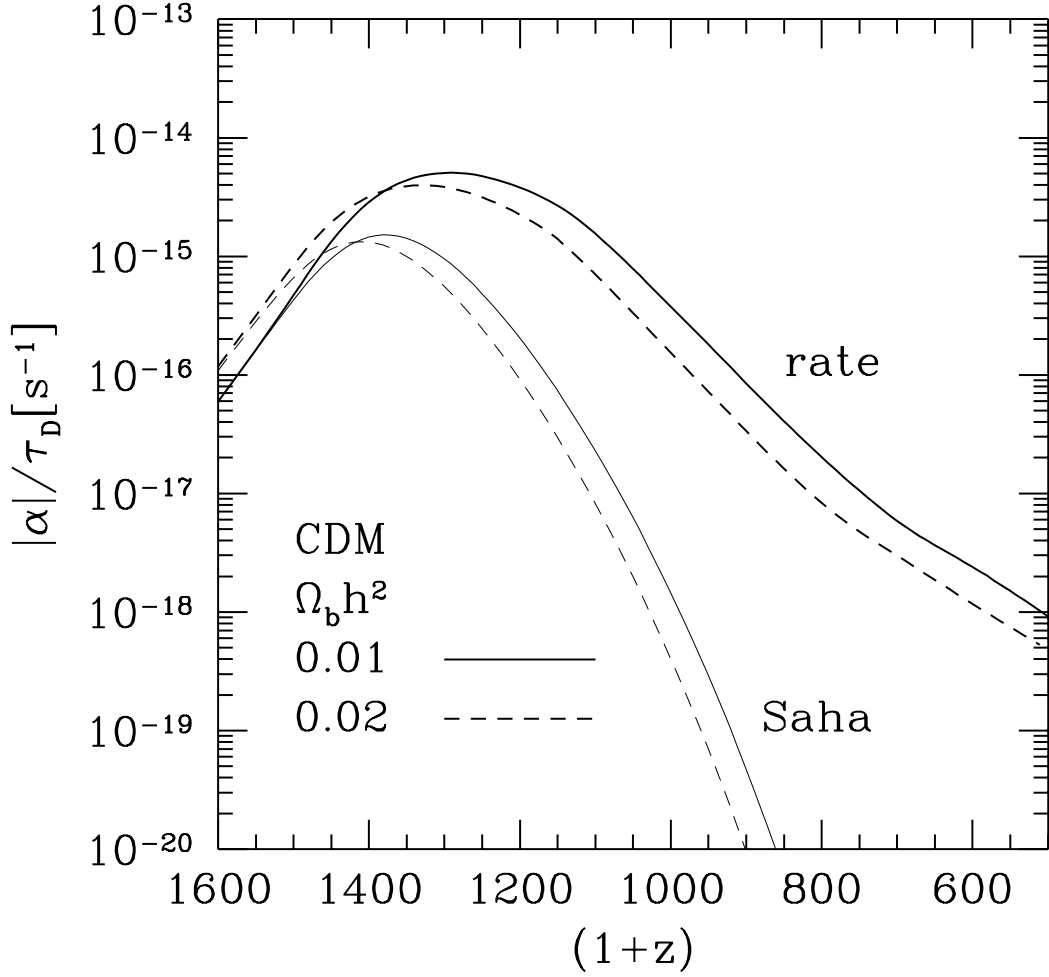


Fig. 9.— Ratio of $|\alpha|$ to τ_D from the rate equation (thick lines) and the Saha equation (thin lines) for the fiducial CDM models $\Omega_0 = 1.0$, $\Omega_b = 0.04$, and $h = 0.5$ (solid lines) and $\Omega_0 = 1.0$, $\Omega_b = 0.08$, and $h = 0.5$ (dashed lines). The ratio depends only on $\Omega_b h^2$ in use of the Saha equation (see eq. [B11] and eq. [17]) but also depends weakly on Ω_0 in use of the rate equation. The quasi-nonlinear radiation drag force is proportional to $|\alpha|/\tau_D$.

nonlinear mechanism works until later epoch ($z \sim 800$) with the rate equation due to the residual \bar{x}_e and δx_e .

REFERENCES

- Fukugita, M. & Kawasaki, M. 1994, MNRAS, 269, 563
- Gnedin, N. Y., & Ostriker, J. P. 1997, ApJ, 486, 581
- Jones, B.J.T & Wyse, R.F.G., 1985, Astron. Astrophys. 149, 144
- Nishi, R., Susa, H., Uehara, H., Yamada, M., & Omukai, K., 1998, Prog. Theor. Phys., 100, 881
- Ostriker, J. P. & Gnedin, N. Y., 1996, ApJ, 472, L63
- Peebles, P.J.E., 1993, in *Principles of Physical Cosmology* (Princeton University Press, Princeton, New Jersey)
- Peebles, P.J.E., 1968, ApJ, 153, 1
- Pequignot, D., Petitjean, P. & Boisson, C., 1991 A&A 251, 690
- Sato, H. 1971, Prog. Theor. Phys. 45, 370.
- Shaviv, N. 1998 MNRAS, 297, 1245
- Haiman, Z., & Loeb. A., 1997 ApJ, 483, 21
- Silk, J. 1968, ApJ, 151, 459.
- Weinberg, S. 1971, ApJ, 168, 175.
- Yamamoto, K., Sugiyama, N., & Sato, H., 1997, Phys. Rev. D**56**, 7566 (Paper I)
- Yamamoto, K., Sugiyama, N., & Sato, H. 1998, ApJ, 501, 442 (Paper II)